



Characterization of 10 nm – 10 μm coal dust particles generated by simulated different cutting and drilling parameters: mass concentration distribution, number concentration distribution, and fractal dimension

Jintuo Zhu^{1,2,3} · Menglin Chen^{1,2,3} · Liang Wang^{1,2,3} · Haisong Sun^{1,2,3} · Chenghao Wang^{1,2,3} · Noor Azhar^{1,2,3} · Nkansah Benjamin Oduro^{1,2,3}

Received: 10 April 2023 / Revised: 16 June 2023 / Accepted: 10 August 2023
© The Author(s) 2023

Abstract

Nano-to-micron-sized coal dust can cause coal workers' pneumoconiosis (CWP), and cutting and drilling are the main coal dust-generating processes. Based on a self-developed simulated coal cutting and drilling dust generation system, the effects of cutting parameters (tooth tip cone angle, impact angle, roller rotary speed, cutting speed) and drilling parameters (drill bit diameter, drilling speed) on the mass concentration distribution, number concentration distribution and fractal dimension of 10 nm–10 μm coal dust were investigated. Results show that the mass concentration of 10 nm–10 μm coal dust generated by cutting/drilling peak at 5.7–7.2 μm, while the number concentrations during cutting and drilling respectively peak at 60–90 nm and 20–30 nm. During both cutting and drilling processes, the generated coal dust particles in 10–300 nm account for >90% of the total 10 nm–10 μm coal particles, while PM_{2.5} in PM₁₀ is generally below 18%. It is also found that smaller tooth tip cone angle, larger impact angle, lower roller rotary speed, smaller drill bit diameter, or lower drilling speed can reduce the generation of 10 nm–10 μm coal dust with a fractal dimension of 0.94–1.92. This study reveals the distribution characteristics of nano- to micron-sized coal dust particles under different cutting and drilling parameters, and the research results can serve as reference for adjusting cutting and drilling parameters to lower down the 10 nm–10 μm coal dust generation and thus prevent the CWP.

Keywords Coal cutting and drilling · Coal dust · Nano-to-micron-sized particle · Mass concentration · Number concentration · Fractal dimension

1 Introduction

Coal dust is the inevitable by-product of coal mining activities and is the main occupational hazard in coal mines. Long-term exposure to high concentrations of coal dust can induce CWP and seriously threaten the lives and health of coal miners (Li et al. 2011; Mo et al. 2014; Moreno et al. 2019; Peng et al. 2019; Xie et al. 2022). For example: in China, by the end of 2021, a total of 1.026 million cases of occupational diseases were reported, including 0.916 million cases of occupational pneumoconiosis, accounting for nearly 90% of the total number of occupational diseases and about 60% of the occupational pneumoconiosis cases were CWP (Planning, Development and Information Technology Department 2022; Xie et al. 2021). Coal dust measurement data show that when no effective dust control

✉ Liang Wang
wangliang@cumt.edu.cn

¹ Key Laboratory of Gas and Fire Control for Coal Mines (China University of Mining and Technology), Ministry of Education, 221116 Xuzhou, Jiangsu, China
² National Professional Laboratory for Fundamental Research of Mine Gas and Dust Control Technology, School of Safety Engineering, China University of Mining and Technology, 221116 Xuzhou, Jiangsu, China
³ School of Safety Engineering, China University of Mining and Technology, 221116 Xuzhou, Jiangsu, China

measures are taken, the total coal dust concentration during coal shearer cutting and coal seam drilling can reach 8000 and 2000 mg/m³, respectively (Chen et al. 2019; Zhai et al. 2020; Wu et al. 2022; Zhu et al. 2022), and it is summarized that the coal dust generated by cutting and drilling processes respectively accounts for 46% and 12% of the total dust generated in underground coal mines (Zhou et al. 2018; Zhang et al. 2021a, b, c; Wu et al. 2022). In addition, it is summarized that the concentrations of respirable dust generated by cutting and drilling are 167.9–250.2 mg/m³ (Liu 2019; Zhou et al. 2018; Zhou 2020) and 33.6–61.2 mg/m³ (Jiang et al. 2018; Lv 2012; Sastry 2015), respectively, far exceeding the respirable dust concentrations during many other dust generation processes (Chen 2008; Roy et al. 2011; Bao et al. 2019; Pang 2021), indicating that coal cutting and drilling are also the major sources of respirable coal dust in coal mines. To reduce the large amount of coal dust generated by cutting and drilling, scholars have proposed many engineering prevention and control measures, such as adjusting cutting/drilling parameters and applying coal seam water injection to reduce dust production, exerting high-pressure water spray to capture and remove floating dust, and improving local ventilation to dilute and exhaust dust, etc. (Kim et al. 2017; Xie et al. 2017; Hua et al. 2020; Zhou et al. 2020a, b; Li et al. 2021; Zhang et al. 2021a, b, c, 2022; Nie et al. 2022; Wang et al. 2022). Among them, water-based dust reduction and removal techniques (coal seam water injection, high-pressure water spray, water curtain, etc.) are the current main adopted dust control measures in coal mines (Wang et al. 2019a, b; Wei et al. 2020; Zhou et al. 2020a, b). However, due to the hydrophobicity of coal dust, even when these measures are taken, the coal dust concentration during coal cutting and drilling still far exceeds the related permissible exposure limits (Shi et al. 2019; Wang et al. 2019a, b; Kornev et al. 2021). Therefore, reducing coal dust generation at the source by adjusting cutting and drilling parameters seems to be a potentially promising measure to lower the coal mine dust concentration and thus prevent the CWP.

At present, there are considerable studies on optimizing cutting/drilling parameters aiming to improve cutting/drilling efficiency and reduce machine energy consumption (Liu et al. 2015; Wang et al. 2018; Wang and Su 2019; Fu et al. 2021). In contrast, only a few studies have investigated the effects of cutting/drilling parameters on coal dust generation from the perspective of dust control. Among those studies on cutting/drilling generated coal dust, there are relatively more investigations using numerical simulations and field measurements but fewer studies through physical simulations under controlled laboratory conditions (Xie et al. 2023). Furthermore, while these studies have shown that cutting/drilling parameters (such as roller rotary speed,

cutting speed, drilling speed, etc.) hold significant effects on generated dust concentration, the target/measured coal dust is mostly total dust and/or respirable dust. However, recent studies have already proved that at the same mass concentration, nano-to-micron-sized coal dust particles are more likely to cause pneumoconiosis due to their smaller size, longer residence time in the air, and higher deposition in the human respiratory system. Moreover, it was found that the deposition rates in the alveolar of 10 nm, 100 nm, 1 μm and 10 μm coal particles were about 40%, 15%, 9% and 1%, respectively, indicating that the smaller the particle size, the higher the deposition rate in the alveolar region (Liu and Liu 2020; Maynard and Kuempel 2005; Shekarian et al. 2021; Yu et al. 2009). Moreover, the latest studies have further revealed that for nanoscale particles, compared with the mass concentration, their number concentration is more closely related to human respiratory diseases (Maynard and Kuempel 2005; Oberdörster et al. 2005; Nho 2020), the study found that with the increase of dust particle size, the possibility of dust entering the lungs becomes smaller. Almost all of the small particles (less than 10 nm) and more than 75% of the large particles (10 μm) are inhalable, with about 20% of the small particles and almost all of the large particles deposited in the head area. Nearly 42% of small particles and about 2% of large particles were deposited in the alveolar area. (Hinds 1999; Ohsaki et al. 2019; Sturm, 2019; Khac et al. 2020; Shekarian et al. 2021). Given the above, there is an urgent need to study both the mass and number of concentrations distribution of nano-to-micron-sized coal dust particles under different cutting/drilling parameters to find suitable parameters to reduce the generation of the coal dust, which is the main threat to the respiratory health of coal miners.

Since particles are usually irregular and have a complex size distribution, the fractal theory is used to study highly non-uniform and complexly varying systems (Mandelbrot 1982; Xie 1992; Ai et al. 1999; Yu et al. 2004). More and more scholars have begun to apply the fractal dimension to quantitatively characterize the complexity of the distribution of coal particles generated under various destruction conditions (Cui et al. 2006; Li et al. 2012a, b; Chu et al. 2017; Qiao 2017; Xu et al. 2021). However, the literature review shows that there is still a research gap in the fractal dimension of 10 nm–10 μm coal dust particles generated in the coal cutting/drilling processes.

To address the above research gaps, based on the similarity criterion and under the controlled laboratory experimental condition, this study self-developed a simulated coal cutting and drilling dust generation system and selected tooth tip cone angle, impact angle, roller rotary speed, and cutting speed as cutting variables, and drill bit diameter and drilling speed as drilling variables. The effects of these

Table 1 Combination of experimental conditions for different simulated coal cutting parameters

Cutting parameters	With tooth tip cone angle as the variable	With impact angle as the variable	With roller rotary speed as the variable	With cutting speed as the variable
Tooth tip cone angle (°)	87	87	87	87
	100			
	110			
Impact angle (°)	90	90	90	90
		75		
		60		
		45		
Rotary speed (r/min)	40	40	40	40
			70	
			100	
			130	
Cutting speed (mm/min)	100	100	100	50
				100
				150
				200
				250

parameters/variables on the mass concentration distribution, number concentration distribution, and fractal dimension of 10 nm–10 μm coal dust particles generated during cutting/drilling were investigated. The research results can serve as a reference for the scientific selection of cutting and drilling parameters to reduce the generation of nano-to-micron-sized coal dust particles and thus prevent the occurrence of CWP.

2 Methods

2.1 Coal sample preparation

In this study, lump coal from the fully mechanized coal face of 3₂ coal seam in Qianyingzi underground coal mine in the Huaibei mining area, Anhui, China, was selected as the experimental coal sample, and the coal sample was gas coal with a protodyakonov coefficient of 0.75. The lump coal was collected, sealed and transported to the laboratory in accordance with the China National Standard *Method of Taking Coal Seam Coal Samples* (China Coal Industry Association 2008). Before the experiment, the lump coal was cut and ground into 60 cm × 40 cm × 20 cm rectangular coal blocks.

2.2 Cutting and drilling parameters

2.2.1 Cutting parameters

Based on the similarity theory, the experimental shearer drum was mechanized with a 1600 mm × 1000 mm drum as the prototype and a similarity ratio of 1/10. The diameter of the drum is 160 mm, the cutting depth is 100 mm, the

Table 2 Combination of experimental conditions for different simulated coal drilling parameters

Drilling parameters	With drilling speed as the variable	With drill diameter as the variable
Drilling speed (r/min)	100	100
	150	
	200	
	300	
Drill diameter (mm)	28	28
		32
		42

number of blades is 2, and the lift angle of the spiral blades is 25°. Pick-shaped cutters with tooth tip cone angles of 87°, 100°, and 110° were manufactured and installed with impact angles of 45°, 60°, 75°, and 90° (see Table 1). The picks are sequentially arranged, and the cutters are evenly installed in the circumferential direction with a cutting line spacing of 10 mm. During the coal-cutting process, the roller rotary speeds were set to 40, 70, 100, and 130 r/min, and the cutting speeds were set to 50, 100, 150, 200, and 250 mm/min (see Table 1).

2.2.2 Drilling parameters

During coal mining, gas extraction and coal seam water injection require the implementation of a large number of coal seam boreholes, and the coal drill bit is the most commonly used drill bit in the process of coal seam drilling (Lu et al. 2011). In this study, diamond composite sheet coal drill bits with diameters of 28, 32, and 42 mm were selected as drilling tools, and the drilling speeds were set to 100, 150, 200, and 300 r/min, respectively (see Table 2).

2.3 Simulated coal cutting and drilling dust generation system

Figure 1 shows the simulated coal cutting and drilling dust generation system, consisting of the experimental chamber, the ventilation unit, the simulated cutting/drilling dust generation unit, the automatic cutting/drilling unit, and the coal dust concentration measurement unit. As presented in Fig. 1, the top and bottom panels of the experimental chamber are used to fix the rectangular coal block prepared in Sect. 2.1; the rear sidewall is airtight, and the front sidewall has holes for the cutting/drilling equipment to probe into, and the left and right sides are built of high-efficiency particulate air (HEPA) filters. The ventilation system consists of a fan and a uniform airflow hood, with the hood connected to the HEPA filter on one side of the chamber, together with the fan to provide a stable, clean airflow in the chamber and to simulate the ventilation of an underground coal mine to remove the continuously generated coal dust during coal cutting and drilling in a timely manner and prevent dust accumulation in the chamber. According to the wind speed requirement for coal mining working faces in the 2022 version of China's *Coal Mine Safety Regulation* (State Administration of work safety, 2022), the fan was adjusted to form a 0.3 m/s airflow inside the chamber. The simulated cutting/drilling dust generation unit consists of the motor guide rail, adjustable motor bracket, variable-frequency motor, and cutting/drilling equipment. Based on programmable logic controller (PLC) technology, the automated cutting/drilling operation unit can realize control of the operating parameters of the simulated cutting/drilling dust generation unit,

such as the movement of the cutting/drilling equipment in three degrees of freedom by automatically jointly adjusting the motor guide rail and the adjustable motor bracket, and the control of the cutting/drilling and rotation speeds by the automated adjustment of the variable-frequency motor. The coal dust concentration measurement unit uses a Scanning Mobility Particle Sizer (SMPS, Model 3910, TSI Inc, Shoreview, MN, USA) and Optical Particle Sizer (OPS, Model 3330, TSI Inc, Shoreview, MN, USA) to work jointly to measure the mass and number of concentrations distribution of 10 nm–10 μm coal dust particles generated under different cutting and drilling parameters. This particle size range covers nano-to-micron-sized coal dust that has the most significant impact on the air pollution in underground coal mines and poses the biggest threat to the respiratory health of coal miners.

2.4 Experimental scheme

Before each experiment, the whole chamber and all related experimental equipment/devices were thoroughly cleaned to avoid any deposited dust interfering with the measurement of the newly generated coal dust. During the experiment, the automated cutting/drilling operation unit was used to control the coal cutting/drilling at pre-set parameters. The coal dust concentration was continuously measured with the monitoring probes arranged on the side of the drum/drill (see Fig. 1). In the pre-experiment, it was found that the coal dust concentration in the chamber stabilized after 2 min of coal cutting/drilling. Therefore, the time to start recording the coal dust concentration was set after 2 min of cutting/

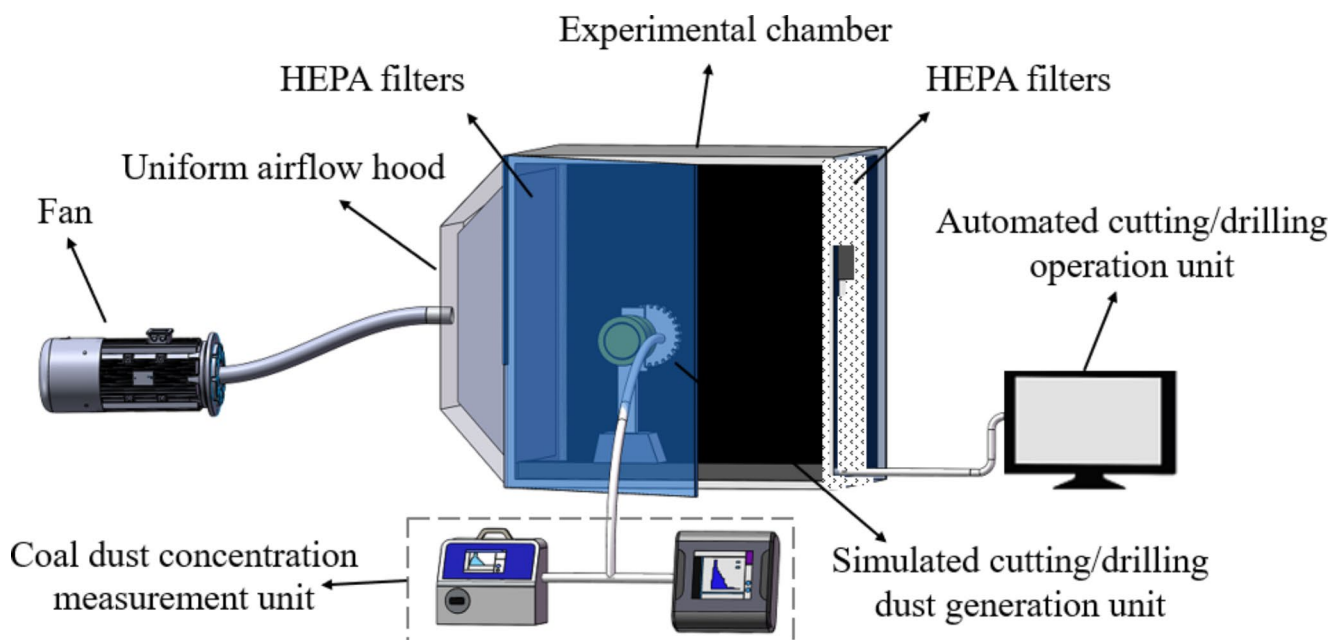


Fig. 1 Simulated coal cutting and drilling dust generation system

drilling, and the monitoring time duration was 3 min. The cutting/drilling parameters were set by the control variable method during the experiment.

2.5 Data process

The data measured by SMPS and OPS was fitted with the built-in function of TSI-MIM2 to obtain the mass and number concentration distribution of 10 nm–10 μm coal dust particles. The PM2.5 and PM10 coal dust mass concentrations and the mass fraction of PM2.5 in PM10 (PM2.5/PM10) were estimated. Finally, the cumulative mass and number distributions of 10 nm–10 μm coal dust particles were obtained from the mass and number concentration distributions, and after the verification of the statistical self-similarity of the coal dust distributions, the cumulative mass and number distributions of coal dust were respectively fitted with the following fractal distribution Eqs. (1) and (2) (Wang et al. 2020). Then the mass fractal dimension (D_M) and number fractal dimension (D_N) were respectively obtained by taking the double logarithm of Eqs. (1) and (2).

$$M(< d) = \alpha d^{3-D_M} \tag{1}$$

$$N(\geq d) = 1 - N(\leq d) = N_0(d/d_{max})^{-D_N} \tag{2}$$

where d is the coal particle size, nm. d_{max} is the maximum coal particle size, nm. α and N_0 are the fitting coefficients for the cumulative mass and number distribution of coal dust, respectively.

3 Results

3.1 Mass and number concentration distribution of 10 nm–10 μm coal dust particles under different cutting parameters

3.1.1 Mass concentration distribution of 10 nm–10 μm coal dust particles

Figure 2 shows the mass concentration distribution of 10 nm–10 μm coal dust particles under different cutting parameters. It can be seen that the mass concentrations of nano-to-micron-sized coal dust generated at different tooth tip cone angles, impact angles, roller rotary speeds, and cutting speeds all exhibit a bimodal distribution of “one small peak+one large peak”, with the small and large peaks occurring at 110–160 nm and 5.7–7.2 μm, respectively. The mass concentrations of coal dust in particle size ranges of 10–50 nm are nearly zero but in the particle size ranges of 60–100 nm and 2–5 μm increase rapidly with increasing

particle size and reach a peak. Overall, the 10 nm–10 μm coal dust mass concentration and its small and large peaks generated in the coal cutting process increase with the increase of tooth tip cone angle and roller rotary speed, but decrease with the impact angle, while are not significantly affected by the cutting speed. In addition, from the comparison of the peak values marked in Fig. 2, it is found that the large peaks at the micron size (551–2065 μg/m³, the large peaks at different levels of the same cutting parameters can be nearly 4 times different) is 50–120 times that of the small peaks at the nano size (10.1–17.5 μg/m³, the peak difference is within 1 time at different cutting parameters). Further statistics revealed that the cumulative mass concentrations of coal dust in the particle size ranges of 10 nm–1 μm and 1 μm–10 μm are 0.216–0.331 and 2.879–7.380 mg/m³, respectively. That is, the mass of micron-sized coal dust generated by cutting was about 13–23 times that of nano-to submicron-sized coal dust.

Figure 3 shows the PM2.5 and PM10 coal dust concentrations and the mass percentage of PM2.5 in PM10 (PM2.5/PM10) under different cutting parameters. As presented, the PM2.5 and PM10 coal dust concentrations generated during coal cutting are 0.51–1.06 and 3.04–7.71 mg/m³, respectively, and the PM2.5/PM10 is within 10.6%–17.8%. In particular, as the tooth tip cone angle was raised from 87° to 110°, PM2.5 and PM10 increased by 43% and 92%, respectively, whereas PM2.5/PM10 reduced from 17.4% to 12.3%. When the impact angle was increased from 45° to 90°, PM2.5 and PM10 decreased by 34% and 60%, respectively, meantime the PM2.5/PM10 increased from 10.6 to 17.7%. When the roller rotary speed was increased from 40 r/min to 130 r/min, PM2.5 and PM10 increased by 103% and 147%, respectively, while PM2.5/PM10 reduced from 17.7% to 14.1%. However, with the increasing cutting speed, no significant change was found in PM2.5, PM10, or PM2.5/PM10.

3.1.2 Number concentration distribution of 10 nm–10 μm coal dust particles

Figure 4 presents the number concentration distribution of 10 nm–10 μm coal dust particles under different cutting parameters. As can be seen, the number concentrations of nano- to micron-sized coal dust generated by coal cutting show a unimodal distribution with the peak value appearing at the particle size of 60–90 nm, and the peak concentrations are in the range of 14,636–22,049 cm⁻³. The differences among different peak values at different levels of the same cutting parameters are within 43% or 6500 cm⁻³. In the particle size range of 10 nm–10 μm, the number concentrations of coal dust increased with the increase of tooth tip cone angle and roller rotary speed, while decreased with

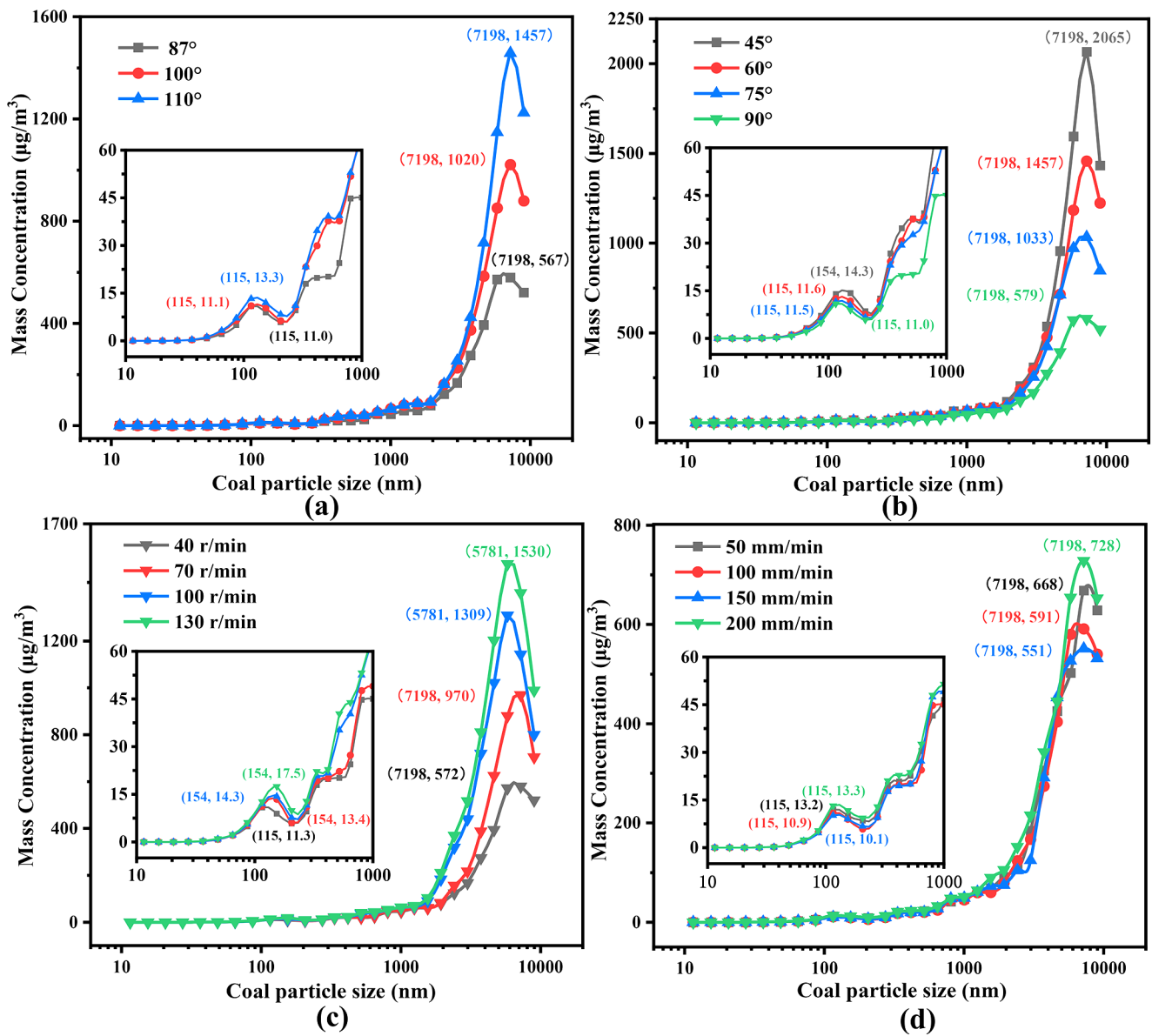


Fig. 2 Mass concentration distribution of 10 nm–10 μm coal dust particles under different cutting parameters **a** Tooth tip cone angle **b** The impact angle **c** Roller rotary speed **d** Cutting speed

the impact angle and did not change significantly with the cutting speed. Further statistics show that the number of coal dust particles in the particle size range of 10–300 nm alone accounts for 90% of the total number of coal dust particles in size range of 10 nm–10 μm.

The reasons for the above characteristics of mass and number concentration distribution of coal dust particles generated under different cutting parameters can be attributed to the following aspects: (1) Tooth tip cone angle. Studies by Roepke and Voltz (1983) and Evans and Ivor (1984) confirmed that the larger the tooth tip cone angle, the larger the area of the compacted coal block at the tooth tip, and the higher the cutting force exerted by the cutting tooth on the

coal, resulting in more coal dust particles generated during the cutting process and correspondingly an increase in the mass and number concentrations of coal dust. Moreover, the larger the tooth tip cone angle, the blunter the tooth. Thus, the tooth's ability to cut coal is weakened, leading to the reduction of PM_{2.5}/PM₁₀. (2) The impact angle. Bilgin et al. (2006) and Park et al. (2018) reported that the increasing impact angle would reduce the contact area between the cutting tooth and the coal body as well as the cutting force exerted by the tooth on the coal body, thus reducing the mass and number concentrations of coal dust generated during coal cutting. (3) Roller rotary speed. Li et al. (2012a, b; Bakhtavar and Shahriar (2013) also found that with the

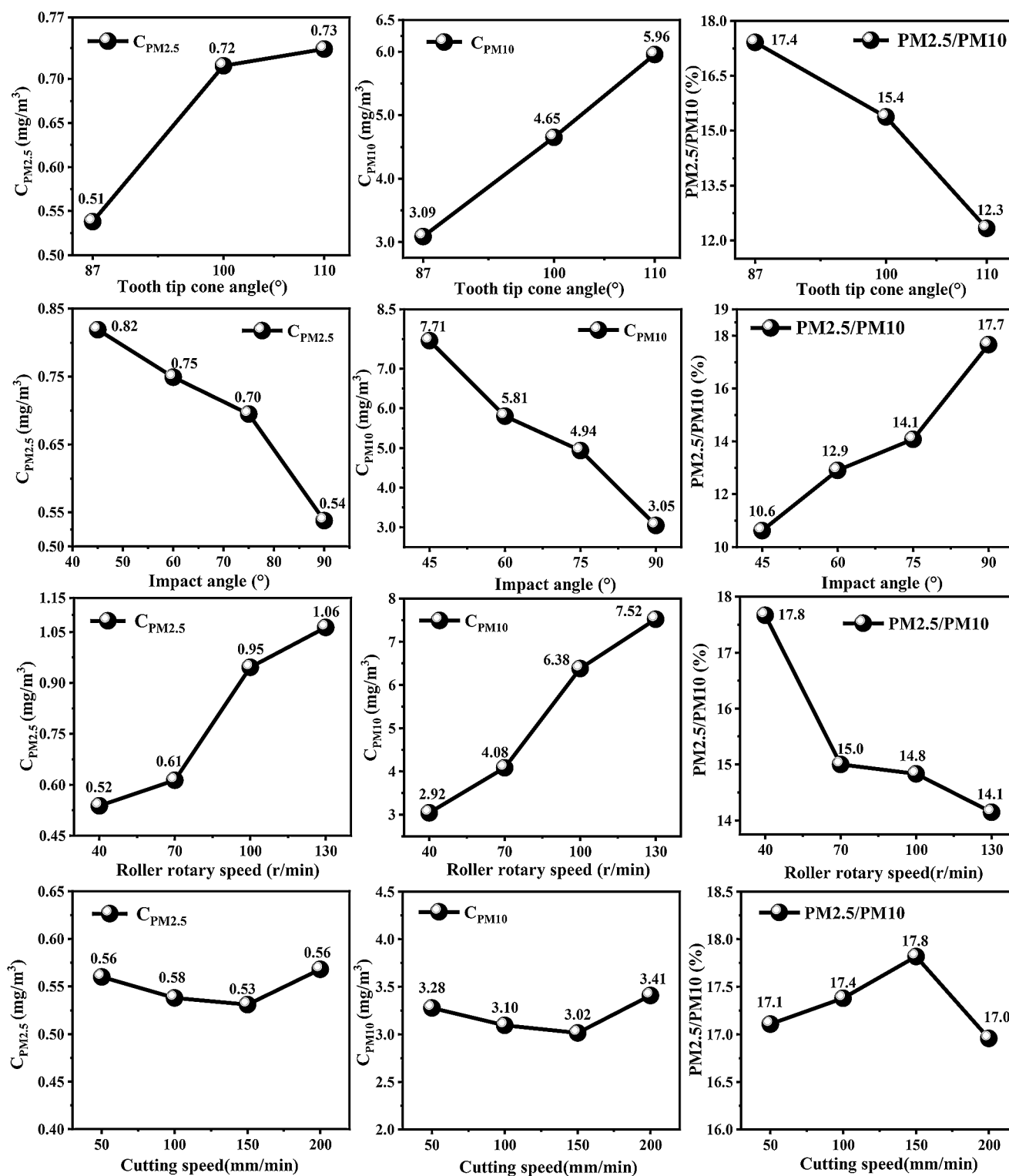


Fig. 3 PM2.5 and PM10 coal dust concentrations and the mass percentage of PM2.5 in PM10 (PM2.5/PM10) under different cutting parameters

increase of roller rotary speed, the concentration of respirable coal dust increased. Through the observation and analysis of the cutting process, this study attributes the increase in the mass and number concentrations of 10 nm–10 μm

coal dust with the roller rotary speed to two aspects: (1) As the increase of roller rotary speed, more cutting teeth are involved in the coal-chopping operations within unit time, which increases the generated coal dust. (2) As the roller

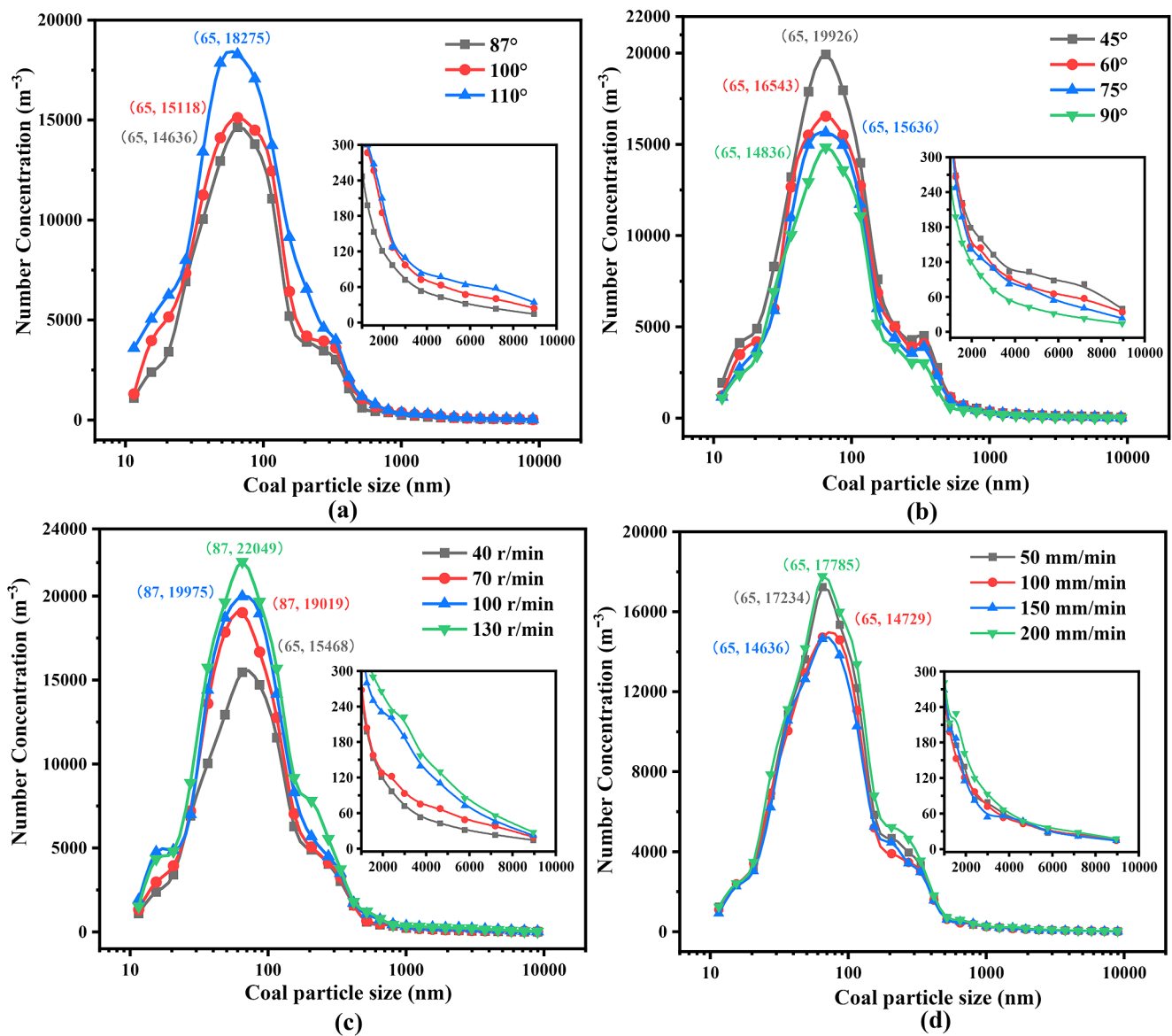


Fig. 4 Number concentration distribution of 10 nm–10 μm coal dust particles under different cutting parameters: **a** Tooth tip cone angle **b** The impact angle **c** Roller rotary speed **d** Cutting speed

rotary speed increases, partially broken coal pieces cannot be promptly discharged from the cutting teeth, which increases collisions between the coal pieces and the cutting teeth and between the coal pieces themselves, thus generating more coal dust particles. The joint action of the above two aspects can lead to a significant increase in the mass and number of concentrations of coal dust. (4) Cutting speed. The dust generation by coal cutting occurs in the mechanical process of crack propagation and breaking of coal under force, while the crack propagation speed is much higher than the cutting speed, thus the cutting speed has little effect on the dust generation during coal cutting. Through horizontal cutting tests on rock, Rostamsowlat (2018) also verified that

the cutting speed has little effect on the contact stress and friction coefficient.

3.2 Mass and number concentration distribution of 10 nm–10 μm coal dust particles under different drilling parameters

3.2.1 Mass concentration distribution of 10 nm–10 μm coal dust particles

Figure 5 shows the mass concentration distribution of 10 nm–10 μm coal dust particles under different drilling parameters. It can be seen that the coal dust mass concentrations under different drill bit diameters and drilling speeds

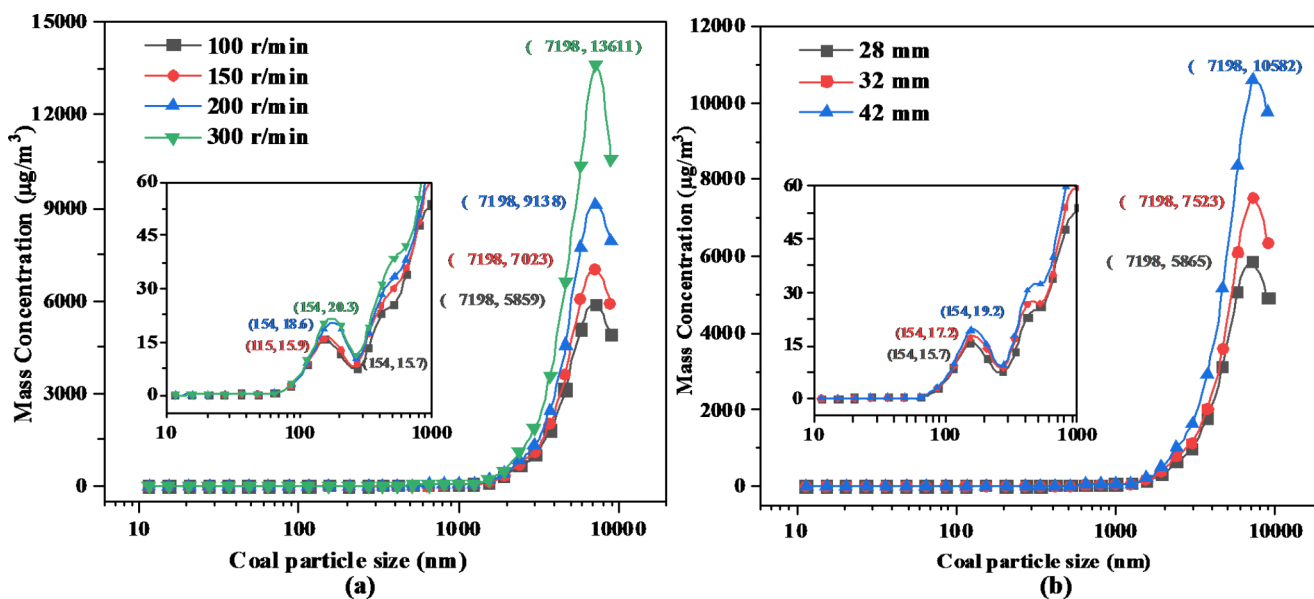
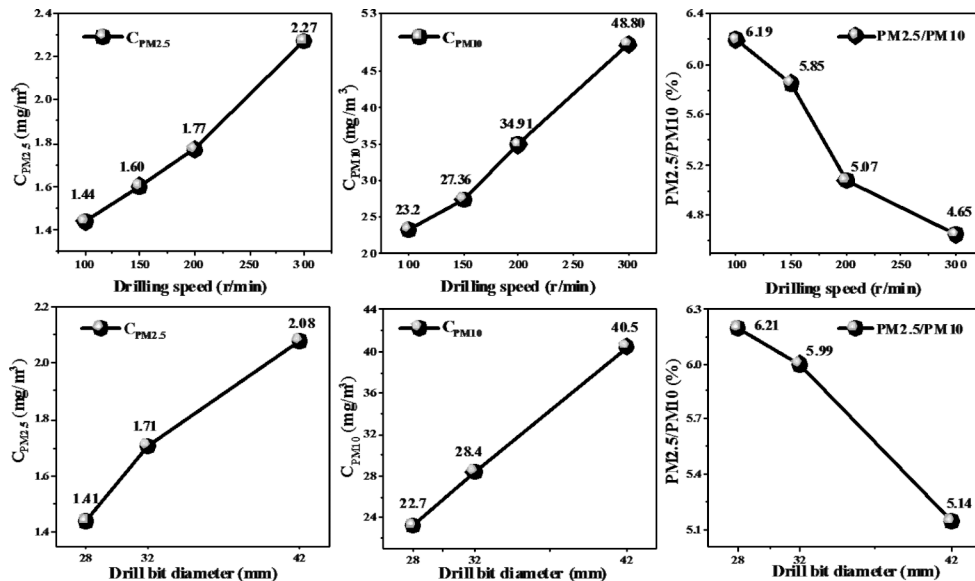


Fig. 5 Mass concentration distribution of 10 nm–10 μm coal dust particles under different drilling parameters a Drilling speed b Drill bit diameter

Fig. 6 PM_{2.5} and PM₁₀ coal dust concentrations and the mass percentage of PM_{2.5} in PM₁₀ (PM_{2.5}/PM₁₀) under different drilling parameters



present a bimodal distribution of “one small peak+one large peak”, with the small and large peaks occurring at 110–160 nm and 7.1–7.2 μm, respectively. The coal dust concentrations were close to zero in the particle size range of 10–70 nm, and increased rapidly to the peak with particle size in the ranges of 90–150 and 200 nm–7 μm. Moreover, with the increase of drill bit diameter and/or drilling speed, this increasing rate and peak values increased significantly. From the peak values marked in Fig. 5, it is found that the large peak concentrations at the micron particle size (5859–13,611 μg/m³, the peak values at different levels of the same drilling parameter can vary by more than 2 times) are 300–700 times higher than the small peak concentrations at the nanoparticle size (15.7–20.3 μg/m³, the peak values

at different drilling parameters vary within 5 μg/m³). Further statistics revealed that the cumulative mass concentrations of coal dust in the particle size ranges of 10 nm–1 μm and 1 μm–10 μm are 0.24–0.33 and 22.96–58.50 mg/m³, respectively, i.e., the mass of micron coal dust generated by drilling is around 90–180 times that of nano- to submicron coal dust.

Figure 6 shows the PM_{2.5} and PM₁₀ coal dust concentrations and PM_{2.5}/PM₁₀ under different drilling parameters. As presented, the PM_{2.5} and PM₁₀ coal dust concentrations generated by drilling are 1.41–22.70 and 22.7–48.8 mg/m³, respectively, and the PM_{2.5}/PM₁₀ is 4.65%–6.21%. Specifically, when the drill bit diameter was increased from 28 to 42 mm, the PM_{2.5} and PM₁₀ generation increased

by 109% and 110%, respectively, while the PM_{2.5}/PM₁₀ reduced from 6.19% to 4.65%. When the drilling speed was increased from 100 r/min to 300 r/min, the PM_{2.5} and PM₁₀ coal dust concentrations increased by 47% and 78%, respectively, while the PM_{2.5}/PM₁₀ reduced from 6.21% to 5.14%.

3.2.2 Number concentration distribution of 10 nm–10 μm coal dust particles

Figure 7 shows the number concentration distribution of 10 nm–10 μm coal dust particles under different drilling parameters. It is found that the coal dust number concentrations at different drill bit diameters and drilling speeds show a bimodal distribution of “one big peak + one small peak”, with the peaks occurring at 20–30 nm and 110–120 nm, respectively. In the particle size range of 10 nm–10 μm, the number concentration increases significantly with the increase of drill bit diameter and/or drilling speed. Unlike the coal-cutting process (see Sect. 3.1.2), the coal dust particles generated by drilling are mainly concentrated in the particle size ranges of 10–40 nm and 70–300 nm, accounting for 63% and 25% of the 10 nm–10 μm total coal particles, respectively.

The main reasons why both mass and number concentrations of nano- to micron-sized coal dust increased with increasing drill bit diameter and drilling speed were: (1) The increase in drilling speed increases the amount of broken coal by the drill bit and the number of coal-block collisions per unit time, increasing the amount of dust generated within unit time and a corresponding increase in coal dust concentration (Tang et al. 2019). Jiang et al. (2018) also reported that increasing the drilling rate would increase

respirable coal dust concentration. (2) With the increase of the drill bit diameter, the contact area between the drill bit and the coal body increases, thus the amount of coal broken by the drill bit per unit time increases, which creates more coal dust around the borehole.

3.3 Fractal dimension of 10 nm–10 μm coal dust particles generated under different cutting and drilling parameters

Figure 8 presents the mass fractal dimension (D_M) and number fractal dimension (D_N) of 10 nm–10 μm coal dust particles under different cutting and drilling parameters, and the correlation coefficients R^2 (generally > 0.95) presented in Fig. 8 confirms that the cumulative mass and number distributions of coal dust fit the Eqs. (1) and (2) well. As can be seen, the D_M under different cutting and drilling parameters are 1.55–1.86 and 1.05–1.22, respectively, and the D_M decreases with the increase of tooth tip cone angle, roller rotary speed, cutting speed, drill diameter, and/or drilling speed, while it tends to increase with impact angle. The D_N under different cutting and drilling parameters are 1.23–1.92 and 0.94–1.33, respectively. In addition, it is found that the D_N decreases with increasing tooth tip cone angle, roller rotary speed, drill diameter and/or drilling speed, and it first decreases significantly, then slowly increases with increasing impact angle but fluctuates up and down with increasing cutting speed.

The data above demonstrate that the D_M and D_N of 10 nm–10 μm coal dust particles generated by coal seam cutting are much higher than those generated by coal drilling. In contrast, the D_M and D_N for coal particles generated by either cutting or drilling are not statistically different.

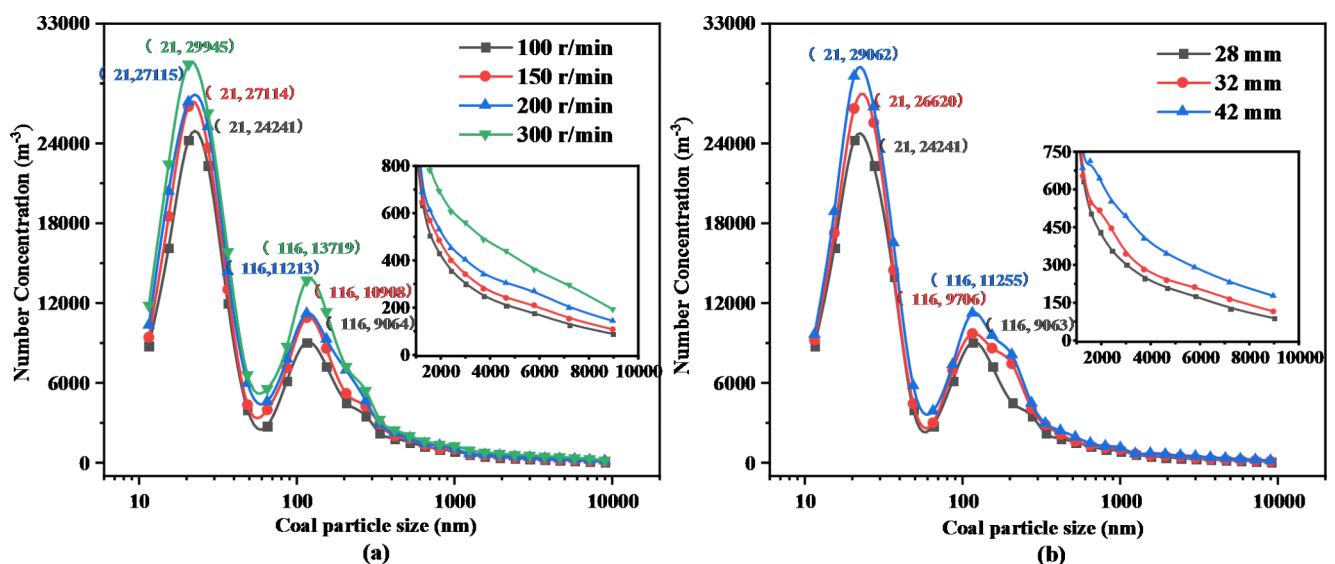


Fig. 7 Number concentration distribution of 10 nm–10 μm coal dust particles under different drilling parameters a Drilling speed b Drill bit diameter

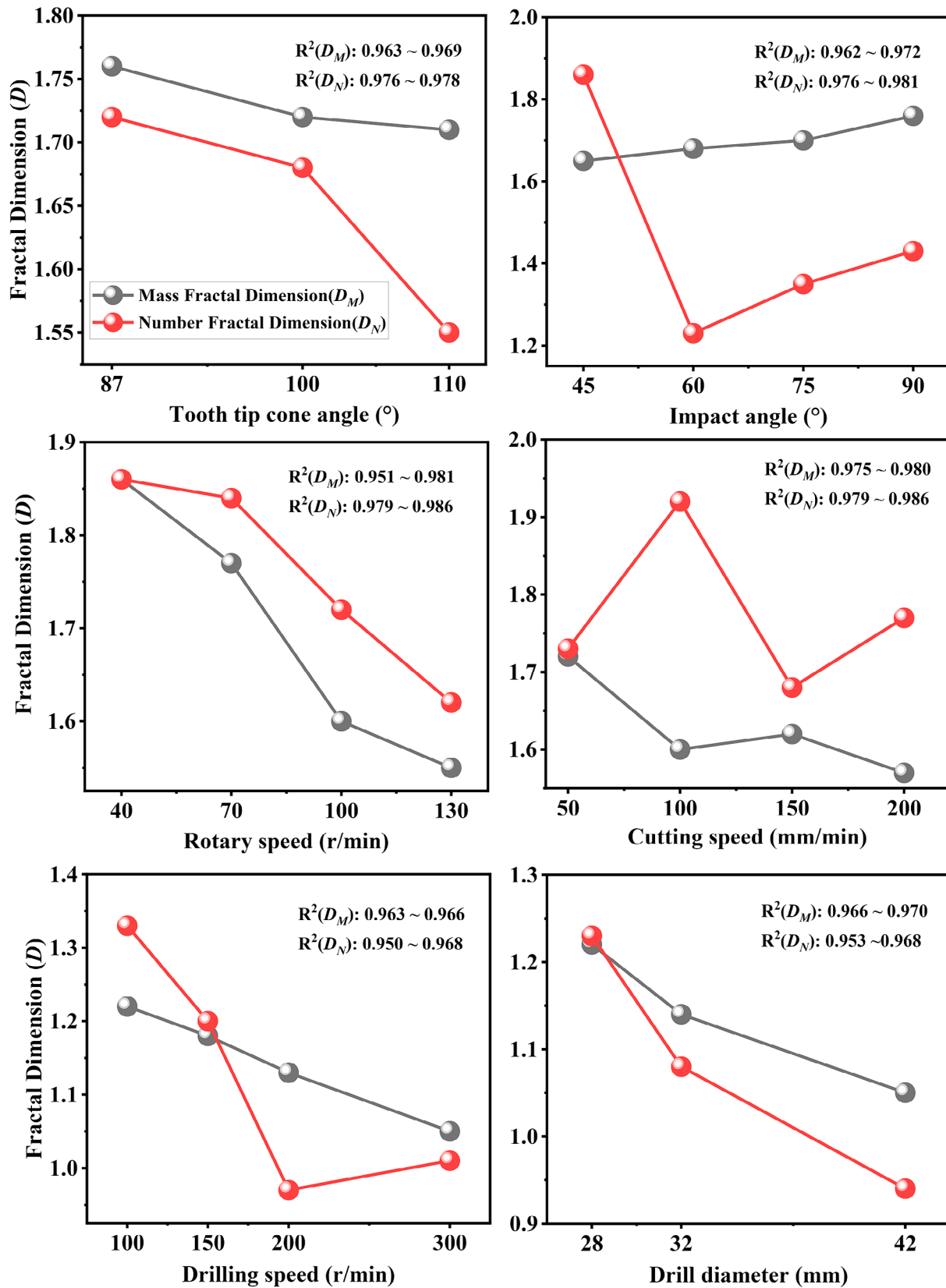


Fig. 8 Fractal dimension of 10 nm–10 μm coal dust particles under different cutting and drilling parameters

Table 3 Fractal dimension of coal particles generated under different destruction conditions

Coal matrix	Destruction conditions	d_{50} (μm)	Mass fractal dimension	Reference
Coal particle	Shearer crushing	11.15	2.50	Li et al.(2012)
Coal particle	cutting	20	1.67	Qiao (2017)
Coal soot	Combustion	46.92	2.20	Chu et al. (2017)
Coal particle	Water jet crushing	123.75	2.80	Cui et al.(2006)
Coal block	Crushing	2030	2.63	Xu et al.(2021)
Coal particle	cutting	3280	2.66	Qiao (2017)

Notes: d_{50} denotes the particle size when the cumulative particle size distribution percentage of dust reaches 50%

The above findings indicate that the distribution of nano-to-micron-sized coal dust particles in the cutting process is more complex than that of the drilling process, while the D_M and D_N are consistent in quantifying the complexity of the distribution of 10 nm–10 μm coal dust particles. When the shearer cuts the coal, the coal body contacting the cutter teeth is first crushed into fine chips and then flaked off from the coal wall under the joint action of shear force, squeezing force and impact force, and this process is called crushing. After two to three times of crushing, larger coal block is cut off (Liu 2012; Sui 2022). The particle size of coal dust generated during crushing is small, while the particle size of coal dust generated during cutting is large, resulting in a large difference in the particle size of coal dust and a more complex distribution of coal dust. During coal drilling, the drill bit exerts compression force and shear force on the coal, with the compression continuously pushing the tip of the bit into the coal, while the shear uses the tip and edge of the bit to scrape off the coal (Li et al. 2016; Lu et al. 2010). Since the coal dust particles generated by drilling are usually difficult to be timely discharged from the borehole, the coal dust particles that are not discharged in time are fully broken by the drill bit inside the borehole, so the coal dust particles generated by drilling are in smaller size, and therefore the coal dust distribution is relatively uniform.

In addition, the mass fractal dimensions of nano-to-micron-sized (10 nm–10 μm) coal dust particles generated by coal seam cutting and drilling obtained in this study (0.94–1.92) are generally smaller than those of micron-to millimeter-sized (11.15 μm –3.28 mm) coal particles reported in previous studies (1.67–2.80, see Table 3), indicating that compared to the micron-to-millimeter coal particles (> 10 μm) produced by other destruction methods (see Table 3), the 10 nm–10 μm coal dust particles generated by cutting and drilling are more uniformly distributed.

4 Conclusions

(1) In the coal-cutting process, the mass concentration of coal dust presented a bimodal distribution of “one small peak+one large peak”, with peaks appearing at 110–160 nm and 5.7–7.2 μm , respectively, where the large peak is 50–120 times the small peak. By contrast, the coal particle number concentration showed a unimodal distribution with the peak at 60–90 nm, and the number of coal particles in the size range of 10–300 nm accounted for 90% of the total number of 10 nm to 10 μm coal particles.

(2) In the coal drilling process, the mass concentration of coal dust shows a bimodal distribution of “one small peak+one large peak”, with the peaks occurring at 110–160 nm and 7.1–7.2 μm respectively, where the large peak is 300–700 times of the small peak. By contrast, the coal particles number concentration shows a bimodal distribution of “one large peak+one small peak”, with the peaks appearing at 20–30 nm and 110–120 nm, respectively. The number of coal particles in size ranges of 10–40 nm and 70–300 nm respectively accounts for 63% and 25% of the total number of 10 nm–10 μm coal particles.

(3) The generated nano- to micron-sized coal dust particles increases with the increase of tooth tip cone angle, roller rotary speed, drill bit diameter, and/or drilling speed, and decrease with the increase of impact angle, while are not significantly affected by cutting speed.

(4) The mass percentage of PM2.5 in PM10 (PM2.5/PM10) decreases from 17.4%, 17.8%, 6.19% and 6.21%–12.3%, 14.1%, 4.65% and 5.14% with the increase of tooth tip cone angle, roller rotary speed, drilling speed and drill bit diameter, respectively, and increases from 10.6% to 17.7 with the increase of impact angle, while are not significantly affected by cutting speed.

(5) The mass fractal dimensions of 10 nm–10 μm coal dust particles generated by cutting and drilling processes are 1.55–1.89 and 1.05–1.22, respectively, and the corresponding number fractal dimensions are 1.23–1.92 and 0.94–1.33, indicating that the distribution of nano- to micron-sized coal dust particles produced by cutting is more complex than that of drilling. Moreover, compared to the micron-to-millimeter coal particles (> 10 μm) generated by other crushing methods, the 10 nm–10 μm coal dust particles generated by cutting and drilling are more uniformly distributed.

Acknowledgements The authors would like to thank the financial support from the National Natural Science Foundation of China (51904291 and 51974300), the Basic Research Program of Jiangsu Province (BK20190638), Anhui Province Key Laboratory of Human Safety, the Project funded by China Postdoctoral Science Foundation (2020M681781), the Jiangsu Planned Projects for Postdoctoral Research Funds (2020Z076), the Graduate Innovation Program of China University of Mining and Technology (2023WLJCRZL200)

and the Postgraduate Research & Practice Innovation Program of Jiangsu Province.

Authors contribution **Zhu Jintuo**: Conceptualization, Methodology, Writing - Original draft, Writing - Review & Editing, Supervision, Project administration. **Chen Menglin**: Formal analysis, Writing - Original Draft. **Wang Liang**: Resources, Supervision. **Sun Haisong**: Formal analysis, Investigation, Writing - Original Draft. **Wang Chenghao**: Formal analysis. **Noor Azhar**: Methodology. **Nkansah Benjamin Oduro**: Methodology.

Funding This work was supported by the National Natural Science Foundation of China (51904291, 51974300); the Basic Research Program of Jiangsu Province (BK20190638); Anhui Province Key Laboratory of Human Safety, the Project funded by China Postdoctoral Science Foundation (2020M681781); the Jiangsu Planned Projects for Postdoctoral Research Funds (2020Z076); the Graduate Innovation Program of China University of Mining and Technology (2023WLJRCZL200) and the Postgraduate Research & Practice Innovation Program of Jiangsu Province (SJCX23_1313).

Declarations

Competing interests The authors declare that they have no known competing financial interests or personal relationships that could have appeared to influence the work reported in this paper.

Open Access This article is licensed under a Creative Commons Attribution 4.0 International License, which permits use, sharing, adaptation, distribution and reproduction in any medium or format, as long as you give appropriate credit to the original author(s) and the source, provide a link to the Creative Commons licence, and indicate if changes were made. The images or other third party material in this article are included in the article's Creative Commons licence, unless indicated otherwise in a credit line to the material. If material is not included in the article's Creative Commons licence and your intended use is not permitted by statutory regulation or exceeds the permitted use, you will need to obtain permission directly from the copyright holder. To view a copy of this licence, visit <http://creativecommons.org/licenses/by/4.0/>.

References

- Ai NS, Chen R, Li HQ (1999) Towards fractal geomorphology. *Geogr Territorial Res* 1:92–96
- Bakhtavar E, Shahriar K (2013) Selection of a practicable Shearer Loader based on Mechanical Properties of coal for parvadeh 1 mine. *Arch Min Sci* 58(1):145–157. <https://doi.org/10.2478/amsc-2013-0010>
- Bao Q, Nie W, Liu C, Liu Y, Zhang H, Wang H, Jin H (2019) Preparation and characterization of a binary-graft-based, water-absorbing dust suppressant for coal transportation. *J Appl Polym Sci* 136(7):47065. <https://doi.org/10.1002/app.47065>
- Bilgin N, Demircin MA, Copur H, Balci C, Tuncdemir H, Akcin N (2006) Dominant rock properties affecting the performance of conical picks and the comparison of some experimental and theoretical results. *Int J Rock Mech Min* 43(1):139–156. <https://doi.org/10.1016/j.ijrmms.2005.04.009>
- Chen SJ, Chen JS, Li GG, Gao Y, Zhao XF (2019) Numerical simulation of dust concentration distribution regularities during dry drilling in coal seam. *J Harbin Inst Technol* 51(10):123–129
- Chen ZQ (2008) The research on dust prevention and control in the tunnel construction with drilling and blasting method. Dissertation, Shandong University
- China Coal Industry Association (2008) Sampling of coal seams (GB/T 482–2008. China Standard Press, Beijing. (in Chinese)
- Chu HQ, Ren F, Zheng ZM, Gu MY (2017) Study on granularity distribution of powder by Fractal Models. *Fractals* 25(4):1740009. <https://doi.org/10.1142/S0218348X17400096>
- Cui LL, An LQ, Gong WL (2006) Effects of process parameters on the comminution capability of high pressure water jet mill. *Int J Miner Process* 81(2):113–121. <https://doi.org/10.1016/j.minpro.2006.07.005>
- Evans I (1984) Theory of the cutting force for point-attack picks. *Int J Min Eng* 2(1):63–71. <https://doi.org/10.1007/BF00880858>
- Fu MX, Liu SW, Jia HS, Zhang WG (2021) Generation mechanism and size characteristics of the rock fragments during borehole drilling in coal mine roadway floor. *J China Univ Min Technol* 50(2):228–238
- Hinds WC (1999) *Aerosol technology: Properties, behaviour and measurement of airborne particles*, 2nd ed. John Wiley & Sons, New York, pp 182–205
- <http://www.nhc.gov.cn/guihuaxxs/s3586s/202207/51b55216c2154332a660157abf28b09d.shtml>. Accessed 12 July 2022
- Hua Y, Nie W, Liu Q, Peng HT, Wei WL, Cai P (2020) The development and application of a novel multi-radial-vortex-based ventilation system for dust removal in a fully mechanized tunnelling face. *Tunn Undergr Space Technol* 98:103253. <https://doi.org/10.1016/j.tust.2019.103253>
- Jiang H, Luo Y, McQuerrey J (2018) Experimental study on effects of drilling parameters on respirable dust production during roof bolting operations. *J Occup Environ Hyg* 15(2):143–151. <https://doi.org/10.1080/15459624.2017.1395960>
- Khac V, Bui H, Moon JY, Chae M, Lee YC (2020) Prediction of aerosol deposition in the human respiratory tract via computational models: a review with recent updates. *Atmosphere* 11(2): 137. <https://doi.org/10.3390/atmos11020137>
- Kim E, Hirro K, Oliveira D, Kim A (2017) Effects of the skew angle of conical bits on bit temperature, bit wear, and rock cutting performance. *Int J Rock Mech Min* 100:263–268. <https://doi.org/10.1016/j.ijrmms.2017.11.006>
- Kornev AV, Korshunov GI, Kudelas D (2021) Reduction of Dust in the Longwall Faces of Coal Mines: problems and perspective solutions. *Acta Montan Slovaca* 26(1):84–97. <https://doi.org/10.46544/AMS.v26i1.07>
- Li M, Luo M, Jiang H (2016) Effects of proper drilling control to reduce respirable dust during roof bolting operations. *Int J Coal Sci Technol* 3:370–378. <https://doi.org/10.1007/s40789-016-0154-x>
- Li QZ, Lin BQ, Zhang JK, Dan JJ, Dai HM (2012a) Fractal characteristics of particle size distribution and its effects on the surface wetting performance of coal mine dusts. *J China Coal Soc* 37(1):138–142. <https://doi.org/10.13225/j.cnki.jccs.2012.s1.033>
- Li SG, Zhao B, Lin HF, Shuang HQ, Kong XG, Yang EH (2021) Review and prospects of surfactant-enhanced spray dust suppression: mechanisms and effectiveness. *Process Saf Environ* 154:410–424
- Liu KY (2012) The structure improvement for cutting roller (φ2.0m) of the coal cutting machine. Dissertation, Taiyuan University of Technology
- Liu T, Liu SM (2020) The impacts of coal dust on miners' health: a review. *Environ Res* 190:109849. <https://doi.org/10.1016/j.envres.2020.109849>
- Liu XH, Liu SY, Tang P (2015) Coal fragment size model in cutting process. *Powder Technol* 272:282–289. <https://doi.org/10.1016/j.powtec.2014.12.015>

- Liu ZJ (2019) Study on dust distribution characteristics and control technology of fully mechanized working face in Hongliulin coal mine. Dissertation, Xi'an University of Science and Technology
- Li XH, Liu SM, Huang ZL, Du W (2012b) Study of the Effects of Shearer's kinematic parameters on On-way distribution of Dust on Coal Face. *Appl Mech Mater* 127:400–405. <https://doi.org/10.1016/j.psepe.2021.08.037>
- Li YQ, Qin YP, Yang XB, Liang T (2011) New progress on coal mine dust in recent ten years. *Procedia Eng* 26:738–743. <https://doi.org/10.1016/j.proeng.2011.11.2231>
- Lu YY, Liu Y, Li XH, Kang Y (2010) A new method of drilling long boreholes in low permeability coal by improving its permeability. *Int J Coal Geol* 84(2): 94–102. <https://doi.org/10.1016/j.coal.2010.08.009>
- Lu YY, Wang J, Jiang LY, Kang Y, Xia BW (2011) Design and experimental study of drilling hole dust collector apparatus used in coal drilling. *J China Coal Soc* 36(10):1725–1730. <https://doi.org/10.13225/j.cnki.jccs.2011.10.032>
- Lv YC (2012) Application of water jet vacuum ejector dust technology in coal mine methane drainage drilling of wind row powder. Dissertation, China University of Mining and Technology
- Mandelbrot BB (1982) *The fractal geometry of nature*. WH freeman, New York
- Maynard AD, Kuempel ED (2005) Airborne nanostructured particles and occupational health. *J Nanopart Res* 7:587–614. <https://doi.org/10.1007/s11051-005-6770-9>
- Mo JF, Wang L, Au W, Su M (2014) Prevalence of coal workers' pneumoconiosis in China: a systematic analysis of 2001–2011 studies. *Int J Hyg Envir Heal* 217(1):46–51. <https://doi.org/10.1016/j.ijheh.2013.03.006>
- Moreno T, Trechera P, Querol X, Lah R, Johnson D, Wrana A, Williamson B (2019) Trace element fractionation between PM10 and PM2.5 in coal mine dust: implications for occupational respiratory health. *Int J Coal Geol* 203:52–59. <https://doi.org/10.1016/j.coal.2019.01.006>
- Nho R (2020) Pathological effects of nano-sized particles on the respiratory system. *Nanomed-Nanotechnol* 29:102242. <https://doi.org/10.1016/j.nano.2020.102242>
- Nie W, Sun N, Liu Q, Guo LD, Xue QQ, Liu CY, Niu WJ (2022) Comparative study of dust pollution and air quality of tunnelling anchor integrated machine working face with different ventilation. *Tunn Undergr Sp Tech* 122:104377. <https://doi.org/10.1016/j.tust.2022.104377>
- Oberdörster G, Oberdörster E, Oberdörster J (2005) Nanotoxicology: an emerging discipline evolving from studies of ultrafine particles. *Environ Health Persp* 113(7):823–839. <https://doi.org/10.1289/ehp.7339>
- Ohsaki S, Mitani R, Fujiwara S, Nakamura H, Watano S (2019) Effect of particle-wall interaction and particle shape on particle deposition behavior in human respiratory system. *Chem Pharm Bull* 67(12): 1328–1336. <https://doi.org/10.1248/cpb.c19-00693>
- Pang XY (2021) Research on dust production law of belt conveyor and automatic spray dust suppression technology in preparation workshop. Dissertation, Liaoning Technical University
- Park JY, Kang H, Lee JW, Kim JH, Oh JY, Cho JW, Kim HD (2018) A study on rock cutting efficiency and structural stability of a point attack pick cutter by lab-scale linear cutting machine testing and finite element analysis. *Int J Rock Mech Min* 103:215–229. <https://doi.org/10.1016/j.ijrmm.2018.01.034>
- Peng HT, Nie W, Cai P, Liu Q, Liu ZQ, Yang SB (2019) Development of a novel wind-assisted centralized spraying dedusting device for dust suppression in a fully mechanized mining face. *Environ Sci Pollut R* 26:3292–3307. <https://doi.org/10.1007/s11356-018-3264-8>
- Planning, Development and Information Technology Department (2022) *Statistical Bulletin on the Development of China's Health Industry in 2021*. Chinese government website
- Qiao SC (2017) Study on the Regularity of Dust and Dust Characteristics of Fragile Coking Coal. Dissertation, Shandong University of Science and Technology
- Roepke WW, Voltz JI (1983) Coal cutting forces and primary dust generation using radial gage cutters. Bureau of Mines, Minnesota
- Rostamsowlat I (2018) Effect of cutting tool properties and depth of cut in rock cutting: an experimental study. *Rock Mech Rock Eng* 51(6):1715–1728. <https://doi.org/10.1007/s00603-018-1440-2>
- Roy S, Adhikari GR, Renaldy TA, Jha AK (2011) Development of multiple regression and neural network models for assessment of blasting dust at a large surface coal mine. *J Environ Sci Technol* 4(3):284–301
- Sastry VR, Chandar KR, Nagesha KV, Muralidhar E, Mohiuddin MS (2015) Prediction and analysis of dust dispersion from drilling operation in opencast coal mines. *Procedia Earth Planet Sci* 11:303–311. <https://doi.org/10.1016/j.proeps.2015.06.065>
- Shekarian Y, Rahimi E, Rezaee M, Su WC, Roghanchi P (2021) Respirable coal mine dust: a review of respiratory deposition, regulations, and characterization. *Minerals* 11(7):696. <https://doi.org/10.3390/min11070696>
- Shi GQ, Han C, Wang YM, Wang HT (2019) Experimental study on synergistic wetting of a coal dust with dust suppressant compounded with noncationic surfactants and its mechanism analysis. *Powder Technol* 356:1077–1086. <https://doi.org/10.1016/j.powtec.2019.09.040>
- State Administration of work safety., 2022. *Coal mine safety regulations, 2022 Edition*. Coal Industry Press, Beijing
- Sturm R (2019) Particles in the lungs of patients with chronic bronchitis—part 1: deposition modeling. *J Public Health Emerg* 5: 1–0. <https://doi.org/10.21037/jphe.2019.03.03>
- Sui PF (2022) Study on influence of different coal joint structures on the cutting characteristics of shearer drum. Dissertation, Liaoning Technical University
- Tang JP, Li WJ, Pan YS, Chen S, Ding JH (2019) Experimental study on the influence of drill pipe diameter and drilling velocity on drilling cuttings. *J Min Saf Engineerinh* 36(1):166–174. <https://doi.org/10.13545/j.cnki.jmse.2019.01.022>
- Wang CH, Cheng YP, Yi MH, Lei Y, He XX (2020) Powder mass of coal after impact crushing: a new fractal-theory-based index to evaluate rock firmness. *Rock Mech Rock Eng* 53:4251–4270. <https://doi.org/10.1007/s00603-020-02174-4>
- Wang G, Wang EM, Huang QM, Li SP (2022) Effects of cationic and anionic surfactants on long flame coal seam water injection. *Fuel* 309:122233. <https://doi.org/10.1016/j.fuel.2021.122233>
- Wang PF, Tan XH, Zhang LY, Li YJ, Liu RH (2019b) Influence of particle diameter on the wettability of coal dust and the dust suppression efficiency via spraying. *Process Saf Environ Port* 132:189–199. <https://doi.org/10.1016/j.psepe.2019.09.031>
- Wang PF, Zhang K, Liu RH (2019a) Influence of air supply pressure on atomization characteristics and dust-suppression efficiency of internal-mixing air-assisted atomizing nozzle. *Powder Technol* 355:393–407. <https://doi.org/10.1016/j.powtec.2019.07.040>
- Wang X, Su OK (2019) Specific energy analysis of rock cutting based on fracture mechanics: a case study using a conical pick on sandstone. *Eng Fract Mech* 213:197–205. <https://doi.org/10.1016/j.engfracmech.2019.04.010>
- Wang X, Wang QF, Liang YP, Su O, Yang L (2018) Dominant cutting Parameters affecting the specific energy of selected Sandstones when using conical picks and the development of empirical prediction models. *Rock Mech Rock Eng* 51:3111–3128. <https://doi.org/10.1007/s00603-018-1522-1>
- Wei JP, Jiang W, Si LL, Xu XY, Wen ZH (2020) Experimental research of the surfactant effect on seepage law in coal seam

- water injection. *J Nat Gas Sci Eng* 103:104612. <https://doi.org/10.1016/j.jngse.2022.104612>
- Wu DM, Gao J, Lu K (2022) Dust Control Technology in Dry Directional drilling in soft and broken coal seams. *Energies* 15(10):3804. <https://doi.org/10.3390/en15103804>
- Xie HP (1992) Fractal geometry and its application to Rock and Soil materials. *Chin J Geotech Eng* 01:14–24. <https://doi.org/10.3321/j.issn:1000-4548.1992.01.002>
- Xie JL, Pang JW, Jian J, Li CT (2017) Experimental study on reducing dust at fully mechanized coal mining face by coal seam water injection. *China Saf Sci J* 27(6):151. <https://doi.org/10.16265/j.cnki.issn1003-3033.2017.06.026>
- Xie Y, Cheng WM, Yu HM, Wang YH (2021) Study on spray dust removal law for cleaner production at fully mechanized mining face with large mining height. *Powder Technol* 389:48–62. <https://doi.org/10.1016/j.powtec.2021.04.095>
- Xie ZW, Huang C, Zhao ZT, Xiao YM, Zhao Q, Lin JQ (2022) Review and prospect the development of dust suppression technology and influencing factors for blasting construction. *Tunn Undergr Sp Tech* 125:104532. <https://doi.org/10.1016/j.tust.2022.104532>
- Xie ZW, Ruan C, Zhao ZT, Huang C, Xiao YM, Zhao Q, Lin JQ (2023) Effect of ventilation parameters on dust pollution characteristic of drilling operation in a metro tunnel. *Tunn Undergr Sp Tech* 132:104867. <https://doi.org/10.1016/j.tust.2022.104867>
- Xu DK, Mu CM, Zhang WQ, Li ZQ (2021) Research on Energy Dissipation Laws of Coal Crushing under the Impact loads. *Shock Vib* 2021:1–13. <https://doi.org/10.1155/2021/5563196>
- Yu DX, Xu MH, Yao H, Liu XW, Zhou K, Wen C, Li L (2009) Physico-chemical properties and potential health effects of nanoparticles from pulverized coal combustion. *Chin Sci Bull* 54(7):1243–1250. <https://doi.org/10.1007/s11434-008-0582-0>
- Yu JF, Liu HJ, Li ZX (2004) Research Method of about Fractal feature of the grain size distribution of sandstone. *J China Univ Min Technol* 33(4):480–485. <https://doi.org/10.3321/j.issn:1000-1964.2004.04.026>
- Zhai GD, Zhang WT, Li YZ, Lu XH, Hu WY (2020) Experimental research and numerical simulation of ejector precipitator in a fully mechanized mining face. *Arab J Sci Eng* 45:9815–9833. <https://doi.org/10.1007/s13369-020-04937-1>
- Zhang C, Yuan S, Zhang NN, Li C, Li H, Yang WY (2021a) Dust-suppression and cooling effects of spray system installed between hydraulic supports in fully mechanized coal-mining face. *Build Environ* 204:108106. <https://doi.org/10.1016/j.buildenv.2021a.108106>
- Zhang MR, Li XC, Chen J, Wang L, Hu Y, Tang GW, Bu BL, Deng XM, Pan SY, Ding H (2022) Numerical simulation-based development and field application of trapezoidal air curtain. *Powder Technol* 2022:407. <https://doi.org/10.1016/j.powtec.2022.117661>
- Zhang R, Liu SM, Zheng SY (2021b) Characterization of nano-to-micron sized respirable coal dust: particle surface alteration and the health impact. *J Hazard Mater* 413:125447. <https://doi.org/10.1016/j.jhazmat.2021b.125447>
- Zhang SB, Nie W, Guo C, Peng HT, Ma QX, Xu CW, Zhang H, Liu QY (2021c) Optimization of spray dust suppression device in return air tunnel of a coal mine based on CFD technology. *Build Environ* 2021c:203. <https://doi.org/10.1016/j.buildenv.2021.108059>
- Zhou G, Feng B, Yin WJ, Wang JY (2018) Numerical simulations on airflow-dust diffusion rules with the use of coal cutter dust removal fans and related engineering applications in a fully-mechanized coal mining face. *Powder Technol* 339:354–367. <https://doi.org/10.1016/j.powtec.2018.07.078>
- Zhou G, Zhang QT, Hu YY, Gao DH, Wang SC, Sun B (2020a) Dust removal effect of negatively-pressured spraying collector for advancing support in fully mechanized coal mining face: Numerical simulation and engineering application. *Tunn Undergr Sp Tech* 95:103149. <https://doi.org/10.1016/j.tust.2019.103149>
- Zhou WD (2020) Mechanisms of dust generation cut by pick used in roadheader and application of reducing dust. Dissertation, China University of Mining and Technology
- Zhou WD, Wang HT, Wang DM, Zhang K, Du YH, Yang HS (2020b) The effect of geometries and cutting parameters of conical pick on the characteristics of dust generation: Experimental investigation and theoretical exploration. *Fuel Process Technol* 198:106243. <https://doi.org/10.1016/j.fuproc.2019.106243>
- Zhu JT, He XJ, Wang L, Liao XX, Teng GP, Jing PL (2022) Performance of N95 elastomeric respirators in high humidity and high coal dust concentration environment. *Int J Min Sci Technol* 32(1):215–224. <https://doi.org/10.1016/j.ijmst.2021.11.007>

Publisher's Note Springer Nature remains neutral with regard to jurisdictional claims in published maps and institutional affiliations.